GTA Weldability Studies on High Manganese Stainless Steel

Progress is reported in isolating some of the factors related to variabilities in welding behavior

BY W. S. BENNETT AND G. S. MILLS

ABSTRACT. GTA weldability studies have been conducted on a relatively new austenitic stainless steel of nominal composition 21Cr-6Ni-9Mn-0.3N. The alloy is currently made by three processes; conventional airmelting, vacuum arc remelting (VAR), and electroslag refining (ESR). Each process produces material of somewhat different weldability.

Porosity in airmelted material is related to oxide inclusion level, and nitrogen content while VAR and ESR porosity levels are related to nitrogen only.

Surface roughness and arc stability are strongly influenced by nitrogen in all three types of steel. ESR material has produced much lower depth to width ratios (D/W) than the other two. The cause of the poor D/W is apparently related to the amount of aluminum picked up during the remelting process. The aluminum appears to interact with manganese to produce increased manganese in the arc.

Introduction

High manganese stainless steel is a relatively new austenitic stainless steel with a nominal yield strength at room temperature in the annealed condition of 65,000 psi (44.8 MPa). The alloy has excellent corrosion resistance, equal to or exceeding that of type 304 in most environments. Further, the austenite is extremely stable making the alloy very useful at cryogenic temperatures. This desirable combination of properties has resulted in increasing use of the alloy, especially in the aircraft and nuclear industries.

The chemistry limits for the alloy are shown in Table 1. Considerable solid solution strengthening results from the high nitrogen content. The high chromium content produces the excellent corrosion resistance and the manganese and nitrogen produce the very stable austenite of this alloy.

The alloy is produced by three different melting practices, conventional airmelt, vacuum arc remelt (VAR), electroslag refined (ESR). Each melting process produces material with somewhat different impurity chemistries and different inclusion levels. These chemistry variations plus the high vapor pressure components of the alloy could produce unusual and possibly variable welding behavior.

Early experiments did indeed show quite a variation in welding behavior from one lot of material to another. Some of the components fabricated from this alloy require extremely precise and reproducible weld geometries and low porosity levels. The variations seen from lot to lot far exceeded the tolerances on some of these items. Because of these problems a comprehensive study of the GTA weldability of this alloy was undertaken. Several aspects of the weldability have been found to be somewhat unique and are reported here.

Porosity, Surface Roughness and Arc Stability

Early attempts to GTA weld high manganese stainless steel (HMSS) produced welds with large variations in porosity, surface roughness, and arc stability. Work has continued in an effort to identify both the cause and the extent of these variations.

Experimental Procedures

GTA welds have been made on a number of different geometries using many different conditions. However, for comparison purposes, autogenous welds on 1½ in. (38.1 mm) or 2 in. (50.8 mm) diam bar stock have been made using the conditions shown in Table 2.

After welding, the centers of the bars were bored out leaving a ¼ in. (6.35 mm) thick wall. The cyclinders were then cut perpendicular to the welds and radiographed to reveal the extent of porosity. The radlographs were judged for severity of porosity on a scale of 1 to 5. Welds free of detectable porosity (detectability limits 0.010 in. (0.254 mm) diam) were rated as 1. Welds with 5 or more voids per inch of weld, greater than 0.025 in. (0.635 mm) diam were rated as 5. The other ratings were evenly spaced in between. The same welds were rated for surface roughness on a scale of 1 to 5 with 1 being the smoothest surface. Welds with ratings of 1, 3, and 5 are shown in Fig. 1.

During GTA welding on certain lots of HMSS, much erratic flashing and some expulsion of molten material

The authors are associated with Dow Chemical U.S.A., Rocky Flats Division, Golden, Colorado.

Paper was selected as alternate for the 55th AWS Annual Meeting held at Houston, Texas, during May 6-10, 1974.

Table 1 — Chemistry Limits High Mn Stainless Steel

Element	wt%
Chromium	18.00-21.00
Nickel	5.50- 7.50
Manganese	8.0 -10.0
Silicon	1.00 Max.
Nitrogen	0.15- 0.40
Phosphorous	0.060 Max.
Carbon	0.040 Max.
Sulfur	0.030 Max.

Table 2 — Standard Welding Conditions

Weld current	— 200 A (dcsp)
Electrode type	— EWTh-2 - 3/32 in. diam
Electrode gap	— 0.060 in.
Torch gas	— 20 cfh Ar
Welding speed	— 5 ipm

from the weld pool occurred. When other lots of material were welded, the arc was very stable with no flashing or expulsion. This flashing and expulsion is referred to here as arc instability. The arc stability was rated as good (G), fair (F), or poor (P) based solely on the judgment of the operator. In welds showing high instability, a deposit slowly formed on the tip of the electrode. In some cases this deposit grew to rather large proportions. Figure 2 shows some of the more extreme deposits encountered. These deposits occurred after approximately 28 linear in. (711 mm) of weld at arc currents of 150 A. The tendency for deposit formation was also rated as good, fair, or poor.

Supplementary information has also been obtained on both autogenous and filler metal addition welds over a wide variety of conditions. This information will be discussed where appropriate in the following sections.

Results and Discussion

The results of porosity, surface roughness and arc stability measurements are shown in Table 3. Several items stand out in reviewing Table 3. First, any one measure of weldability is a good indicator of the other three. Second, airmelt material produces consistently poor results. Third, in the remelted heats, poor weldability is associated with high nitrogen content. Fourth, the electrode buildup occurs when the other instabilities are significant.

The arc instabilities appear much like momentary short-circuiting of the electrode to the weld pool; violent flashing, expulsion of metal and often a loud popping sound. However, there is no pickup of tungsten inclusions in the weld metal and apparent-

Fig. 1 — Extent of surface roughness variations with respective ratings

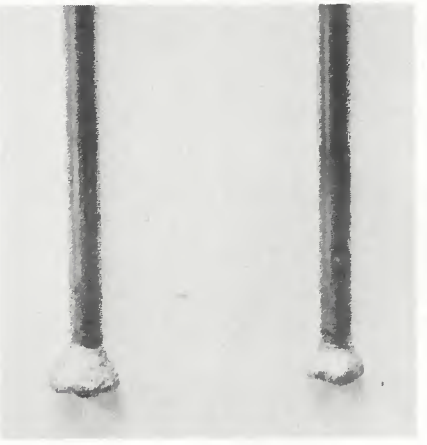

Fig. 2 — Buildup on 3/32 diam electrodes

Fig. 3 — Backscattered electron micrograph of electrode buildup. X100, reduced 38%

Table 3 — Chemistry and Weldability Test Results of General Heats of HMSS

Heat no.	Melt type	N content, wt%	O content, ppm	Porosity rating	Roughness rating	Arc stability	Electrode buildup
81143	VAR	0.30	75	1	2	G	G
81698	"	0.22		1	2	G	G
81942	"	0.28		1	2	G	G
1X0555	"	0.40		5	5	P	F
82287[a]	ESR	0.25		1	1	G	G
82289	"	0.22	55	1	1	G	G
85598	"	0.28		1	1	G	G
6711	"	0.34	30-135	2-3	2	F	F
6818	"	0.39	30	2-3	3-4	P	P
7012-1	"	0.20	30	1	1	G	G
692394	Air	0.38	175	5	5	P	F
680693[a]	"	0.29		4	4	P	F
Welds made with added filler metal							
034037[a]	Air	0.36	260	4			
039038[a]	"	0.38	320	5			
6818W[a]	ESR	0.38	30	1			

(a) Measurements are from specific hardware weldments not standard test bars.

Table 4 — Nitrogen Loss During Welding, wt %

Heat no.	Melt type	N content base metal	N content weld metal	Net loss of nitrogen
1X0555	VAR	0.40	0.35	0.05
81143	VAR	0.30	0.26	0.04
6711	ESR	0.34	0.25	0.09
6818	ESR	0.39	0.26	0.13
82289	ESR	0.22	0.20	0.02

Fig. 4 — Typical inclusion level in an airmelt steel. X100, reduced 27%

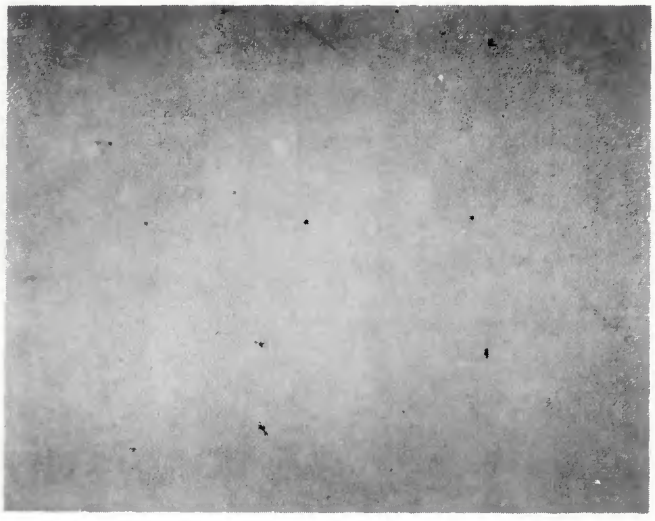

Fig. 5 — Typical inclusion level in an ESR steel. X100, reduced 27%

Fig. 6 — Fine dispersion of inclusions viewed under differential interference contrast lighting. X440, reduced 27%

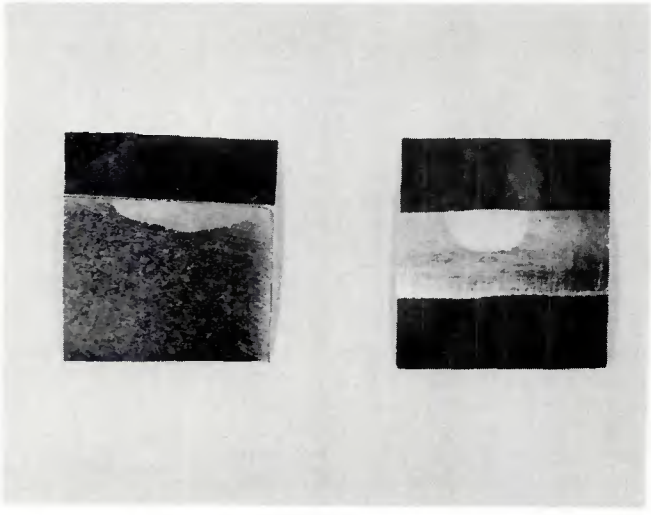

Fig. 7 — Typical fusion zone shapes for a low D/W and a high D/W steel. X2, reduced 27%

ly no actual contact of the weld metal and the electrode. The electrode buildup has been analyzed by microprobe. Figure 3 is a backscattered electron micrograph of a typical region of this deposit. The light colored phase is tungsten and the dark matrix is a mixture of Fe, Cr, and Ni with a trace of Si. The medium colored region surrounding the tungsten particles is a mixture of these two phases.

An additional aspect of weldability is that a second pass made over a weld which previously showed high instability is stable and the surface is smooth. Table 4 gives nitrogen loss during welding for several heats. Although there is nitrogen loss in all cases, the losses are higher in the high nitrogen heats.

These observations suggest that a large quantity of nitrogen is leaving the weld pool. This vapor carries fine droplets of molten steel to the electrode creating the electrode deposit. This droplet laden gas stream may act as a low resistance current path giving the appearance of a momentary short circuit. The arc instability and deposit occur only in the high nitrogen heats, nitrogen >0.3 wt%, and are much worse in those with nitrogen >0.35 wt%.

Brooks (Ref. 1) has studied surface condition and expulsion of electron beam welds versus nitrogen content in HMSS and finds poor surface condition and expulsion are associated with high nitrogen levels. He attributes this behavior to decomposition of chromium nitride inclusions. All of his samples were at the extremes, both high and low, of the nitrogen content for this alloy.

We have examined the microstructure of a number of heats of HMSS to determine the relationship between inclusion levels and GTA weldability. A typical inclusion level for an airmelt heat is shown in Fig. 4, while Fig. 5 shows a typical inclusion level in an ESR heat. The airmelt heat contains 175 ppm oxygen while the ESR heat contains 30 ppm oxygen. Microprobe analysis has shown these inclusions to be of three types; (a) enriched in Mn and S, (b) enriched in Mn, Al, and Si, and (c) enriched in Al only. The last two types are assumed to be oxides and there is general agreement between inclusion content and oxygen level.

In heats with high nitrogen content, a different type of inclusion, a fine dispersion of small particles, occurs, as is shown in Fig. 6. We have been unable to identify these particles due to their small size, but Brooks (Ref. 1) has identified similar particles as chromium nitrides. Further, we have seen them only in heats with nitrogen contents of 0.39 wt% or higher.

At these high nitrogen levels, the

nitride particles apparently decompose, relasing free nitrogen. The porosity could be caused by nitrogen entrapped in the liquid or by nitrogen being expelled at solidification. However, porosity is quite high in the airmelt material even when nitrogen is as low as 0.29 wt%. Further, airmelt filler metal also produces high porosity welds (see Table 3). In airmelt material the oxide inclusions may break down, releasing oxygen and adding to the porosity content. In the remelted material porosity level correlates very well with nitrogen level and porosity is virtually nonexistent when nitrogen is below 0.30 wt%. The extreme surface roughness of the high nitrogen material is apparently caused by agitation of the weld pool as the nitrogen leaves the surface. When a second pass is made over a weld, the nitrogen level is lower, the nitrogen evolved is much less, and the weld surface is smooth and quiet.

Depth to Width Ratio Variations

Another interesting aspect of GTA welding of this alloy has been a large variation in depth of penetration and depth to width ratio (D/W) in autogenous welds. Figure 7 shows the cross section of welds made at the conditions described in Table 2 in two different heats. Several investigators (Refs. 2-4) have reported similar variations in fusion zone geometry. Generally these investigations have related change in geometry with a change in impurity chemistry, but have not resulted in a clear-cut explanation for the variations. We have run a number of experiments to try to find a cause for such behavior.

Experimental Procedures

Autogenous GTA welds have been made on solid bars as described before, under the conditions of Table 2. In addition, arc lengths have been varied from 0.040 to 0.100 in. (1.01 to 2.54 mm), welding speeds from 5 to 20 ipm (127 to 508 mm/min) and torch gas mixtures of 25, 50, and 75% He (balance Ar) have been used. These welds were then sectioned and the depth and width measured.

Several types of chemical analyses have been used to determine the chemical composition of each heat. The major metallic alloying elements have been analyzed using x-ray fluorescence. Oxygen and nitrogen have been analyzed by inert gas fusion. Metallic impurities have been analyzed by emission spectroscopy and spark source mass spectroscopy. Aluminum content has also been measured by atomic absorption spectroscopy.

Spectral analysis of welding arcs was performed in two ways. A GTA welding torch was mounted inside the arc chamber of a standard 3 meter analytical spectrograph and arc spectra were recorded using photographic plates. This technique analyzed light from the entire arc. To analyze light from a specific region of the arc a monochrometer was set up with imaging optics at the inlet slit to focus light from a specific region into the slit. The resulting spectra were then recorded photographically at the exit.

Results and Discussion

Table 5 gives D/W for welds made per conditions of Table 2. The extent of the variations is clearly shown in this table. Several surface preparations (as received, freshly machined, degreased with acetone, etched with inhibited HNO_3) have been used on an ESR heat and a VAR heat with no change in response. Weld samples have been taken from different regions within a bar or plate and again the results are the same. At low welding currents (<50 A) little difference is seen between the heats but at higher currents, the differences show up and persist through 250 A, the highest currents used. Higher welding speeds, up to 20 ipm, have been used and have had little effect on D/W. Electrode tip geometry has been varied from an 18 deg included angle cone to a 120 deg included angle cone with less than 10% change in D/W.

He-Ar torch gas mixtures have improved D/W in the low D/W heats by about 25% with 25% He being nearly as effective as 75% He. The effect of arc length on D/W varied from heat to heat. Figure 8 shows D/W versus arc length for three heats. The curve for the VAR heat is typical for the VAR and airmelt heats while the other curves show the extremes in response for the ESR heats, i.e., some were essentially independent of arc length while others were very sensitive to arc length.

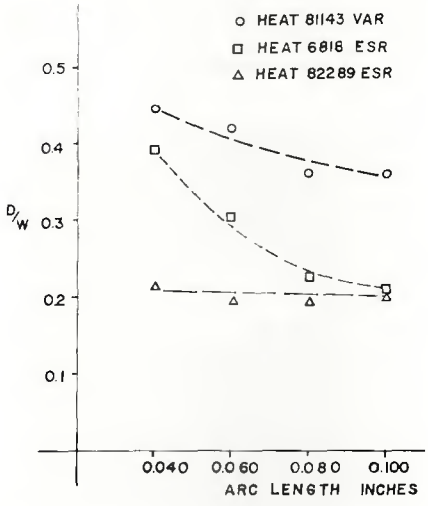

Fig. 8 — Variation in D/W versus arc length for several heats of HMSS

Thermal conductivity changes could explain the variation in D/W even though it seemed unlikely that significant changes could occur. Thermal diffusivity measurements were made at room temperatures and at 600 C on four heats. At room temperature consistent measurements could not be obtained. The 600 C results are shown in Table 6.

The experimental error in these measurements is estimated to be 7% and the results are within 5% so that all four heats have essentially the same value and the D/W variations cannot be explained by thermal conductivity changes.

The only element identified by the various chemical analyses which shows any correlation with D/W is alu-

Table 5 — D/W and Melt Type of Various Heats

Heat no.	Melt type	D/W
81143	VAR	0.45
81698	"	0.57
81942	"	0.57
1X0555	"	0.63
82289	ESR	0.21
85598	"	0.24
6711	"	0.45
6818	"	0.30
7012	"	0.26
82287	"	0.25
692394	Air	0.48

Table 6 — Thermal Diffusivity of Several Heats of HMSS

Heat no.	D/W	Thermal diffus., cm^2/sec
692394	0.48	0.0529
81143	0.45	0.0534
82289	0.21	0.0509
6711	0.45	0.0518

Table 7 — Aluminum Content versus D/W

Heat no.	Melt type	Al content, ppm	D/W
692394	Air	28	0.48
81143	VAR	31	0.45
81698	"	32	0.57
81942	"	27	0.57
1X0555	"	36	0.60
82287	ESR	175	0.25
82289	"	190	0.21
85598	"	96	0.24
6818	"	87	0.30
7012	"	43	0.26
6711	"	30	0.45

minum. No other impurity or alloying elements show any consistent relationship to D/W. The aluminum contents and D/W's are given in Table 7.

These aluminum values are measured by atomic absorption spectroscopy and are the total of soluble plus insoluble aluminum. The various heats fall into two groups; those with D/W's clustered around 0.5 and those clustered around 0.25. Further, all the low D/W heats are ESR processed. Heat 6711 has a higher D/W but was remelted by a slightly different ESR method which minimizes aluminum pickup and it does indeed have a lower aluminum content. The flux used in most ESR operations is a combination of CaO, CaF_2 and Al_2O_3. It has been shown that it is possible to increase the Al content to several times the initial melt amount by reaction with the Al_2O_3 (Ref. 5).

A further check on the effect of aluminum was made by adding aluminum to a weld pool of a heat of steel producing a high D/W. An arc and molten pool were established on a rotating bar and a 0.020 in. (0.508 mm) diam aluminum rod was touched to the edge of the pool. The weld pool instantly widened and the penetration decreased. This behavior persisted for about ½ In. (12.7 mm) of weld at welding speeds of 5 Ipm (127 mm/min). The weld then returned to its original dimensions. This procedure was repeated many times with aluminum additions of about ½ wt% up to 4 wt%. Increasing the amount of aluminum did not change the weld dimensions in the doped area. Further, aluminum additions to 304 stainless steel produced no such change in arc behavior or D/W.

Still photographs have been made of 100 A arcs with 0.060 in. arc lengths. Representative photos are shown in Fig. 9. Photo 9A Is an arc on heat 81698, a VAR heat which produces a high D/W and Photo 9B is an arc on heat 82289, an ESR heat with a low D/W. Note that 81698 produces a typical arc with no unusual features while the arc of 82289 flares out at the workpiece. Further, a dome of light surrounds the arc. Also, 81698, when doped with aluminum as in Fig. 9C, takes on an appearance nearly identical to 82289. Thls dome of light shows up on all the low D/W heats. Color photos show this dome to be a deep blue.

In an attempt to better understand the behavior of various elements in the arc, the llght from the arc was analyzed with the analytical spectrograph mentioned earlier. The hypothesis was that an element peculiar to these heats of steel might be entering the arc In significant quantities and altering the current density of other critical parameter of the arc.

Arc spectra from different heats of steel were recorded on photographic plates and the various elements present were identified by use of available standard plates plus the MIT wavelength tables. All major lines were Identified as elther argon or manganese. The intensities of the impurity element lines were in all cases much less than all but the very weak lines of these two elements. This indicates that the impurities do not affect the energy balance or other physical properties of the arc significantly. A rough determination of the abundance of the alloy elements in the arc indicated that they appear in the order of their vapor pressures: Mn, Cr, Fe, Ni.

Since weld behavior seemed to be correlated with aluminum content, a set of representative lines for the prominent elements plus aluminum were compared on three heats of metal at two different arc currents. The average line intensities from three exposures made as the samples were rotated at a surface speed of 5 ipm (127 mm/min) are show in Table 8.

These data indicate that the variation of alumlnum in the arc does not differ significantly from the variation of the major alloy constituents in the arc. Therefore, the aluminum is not expected to have any more direct effect on the physics of the arc than manganese or chromium.

Examination of arcs with the monochrometer system showed that the deep blue light (described above) is characteristic manganese emission and that a small amount of emission from added aluminum is observed at the surface of the puddle.

Figure 10 shows the spectrum (between 3800 and 4400 angstroms) of light emitted from the area immediately above the molten pool on a low D/W heat. Figure 11 shows the same information for a high D/W heat. The arcs in Figs. 10, 11, and 12 were all run at 100 A, 0.060 in. (1.5 mm) arc length and 5 ipm (127 mm/min) welding speed. The length of the various lines is a measure of the width of the arc over which exitation Is taking place.

Nearly all of the lines visible in these spectra are due to manganese. A comparison of Figs. 10 and 11 with 9A and 9B shows that the extent of manganese emission corresponds to the flare of bright light at the workpiece surface. For comparison, Fig. 12 shows the same spectral region for an arc on 304 stainless steel which is quite similar to Fig. 11. This is in good agreement with their comparative welding behavior.

The spectral information plus other experiments discussed indicates that aluminum and manganese somehow work in combination to decrease the D/W ratio of welds in heats with higher aluminum content. The details of such an interaction are not understood, but are currently the subject of further investigation.

Conclusions

1. The GTA welding behavior of HMSS is quite variable and can be significantly different from that of the more conventional austenitic stainless steels.

2. Porosity, surface roughness, and arc stability of VAR and ESR HMSS welds are strongly related to nitrogen level. These weld properties will be optimized if nitrogen content is

Fig. 9 — Typical arc appearance for a high D/W steel (left), a low D/W steel (center), and a high D/W steel doped with aluminum (right)

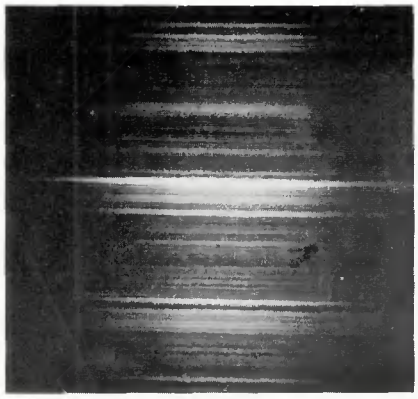

Fig. 10 — Region of spectrum from a weld on a low D/W steel

kept at 0.30 wt% or less.

3. Porosity and surface roughness of welds in airmelt HMSS are worse than in remelted material and apparently are related to both nitrogen level and oxide inclusion level.

4. Welds in ESR material may have much lower penetration and lower D/W than VAR and airmelt material.

5. The lower D/W of ESR welds is related to a higher Al content in the ESR material and seems to be caused by some as yet undefined interaction between aluminum and manganese.

Acknowledgments

The authors wish to acknowledge the assistance of Mr. R. F. Hillyer and Mr. D. H. Riefenberg for the analysis of inclusions and electrode deposits reported. Further, thanks are extended to Mr. R. Acton of Sandia Laboratories for the thermal diffusivity measurements.

The work was performed under Contract AT(29-1)-1106 for the Albuquerque Operations Office of the U.S. Atomic Energy Commission.

Table 8 — Relative Intensities of Representative Lines for Different Steel Samples

Sample no.	Arc current, A	Mn	Fe	Cr	Al
81143	75	2.7	1.0	1.6	0.16
82289	75	10.6	5.5	7.5	1.5
6818	75	6.4	3.1	4.5	0.20
81143	40	2.0	0.9	1.2	0.23
82289	40	4.0	0.7	2.3	2.0
6818	40	3.2	1.0	1.6	0.46

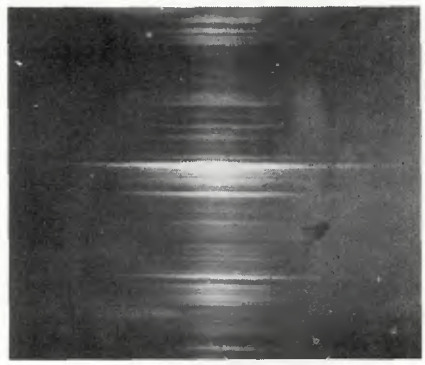

Fig. 11 — Region of spectrum from a weld on a high D/W steel

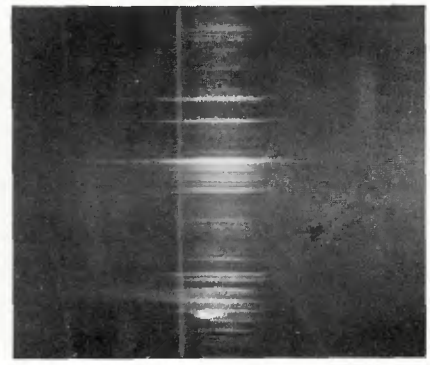

Fig. 12 — Region of spectrum from a weld on 304 stainless steel

References

1. Brooks, J. A., "Electron Beam Weldability of High Nitrogen Stainless Steel," SLL-73-0060, October 1973, Sandia Laboratories.

2. Ludwig, H. C., "Current Density and Anode Spot Size in the Gas Tungsten Arc," *Welding Journal*, 47 (5), May 1968, Res. Suppl., 234-3 to 240-s.

3. Chase, T. F., and Savage, W. F., "Effect of Anode Composition on Tungsten Arc Characteristics," *Welding Journal*, 50 (11), Nov. 1971, Res. Suppl., 467-s to 473-s.

4. Oyler, G. W., Matuszesk, R. A., and Garr, C. R., "Why Some Heats of Stainless Steel May Not Weld," *Welding Journal*, 46 (12), Dec. 1967, 1006 to 1011.

5. Rundell, G. R., Simonds Steel Division, Private Communication.